PHYSICAL REVIEW B **79**, 020502(R) (2009)

Superconductivity without diamagnetism in systems with broken time-reversal symmetry

N. A. Logoboy and E. B. Sonin
Racah Institute of Physics, The Hebrew University of Jerusalem, Jerusalem 91904, Israel
(Received 17 November 2008; published 9 January 2009)

We analyze the phase diagram of superconductors with a broken time-reversal symmetry in an external magnetic field. Ferromagnetism (broken time-reversal symmetry) originates either from the electron spin or the intrinsic angular momentum of Cooper pairs (chiral p-wave superconductors such as Sr_2RuO_4). In addition to the Meissner and the mixed states, the phase diagram includes also the cryptoferromagnetic state with intrinsic domain structure independent of sample shape and size. The cryptoferromagnetic state is not diamagnetic and can be detected by observation of magnetization curves predicted in the present analysis.

DOI: 10.1103/PhysRevB.79.020502 PACS number(s): 74.25.Ha, 74.90.+n, 75.60.−d

In recent years numerous pieces of experimental evidence of superconductivity-ferromagnetism coexistence in various materials were reported.[1–6] Two types of coexistence are possible: (i) the phase transitions to the ferromagnetic and the superconducting (SC) states occur at different temperatures, so the coexistence starts below the lower from the two transitions. Rutheno-cuprates[1] belong to this type: the superconductivity onset occurs at the temperature much lower than the temperature of the magnetic transition. Normally different elements of the crystal structure are responsible for ferromagnetism and superconductivity, and spontaneous magnetization (ferromagnetic order parameter) is related to spin. Later we shall call them spin superconducting ferromagnets (spin SFs). (ii) The magnetic and the SC transitions occur simultaneously. This can take place in unconventional superconductors with triplet Cooper pairing. An example is strontium ruthenate Sr_2RuO_4,[3,4,7–10] where the microscopic theory connects spontaneous magnetization not with the spin but with the orbital intrinsic angular moment of the p-wave Cooper pair with the wave function in the momentum space proportional to p_x+ip_y (chiral p-wave superconductivity). We shall call them orbital superconducting ferromagnets (orbital SFs).

Whereas proof of superconductivity in SFs is quite straightforward, a clear-cut detection of the ferromagnetic order parameter is much more problematic. The internal magnetic field is screened out by the SC Meissner currents and can be present only near sample borders and defects, in particular, domain walls (DWs). This strongly suppresses the stray magnetic fields around the sample, which are most convincing evidence of ferromagnetism. Especially worrying is the situation with strontium ruthenate Sr_2RuO_4, where Kirtley *et al.*[10] could not detect any stray field from DWs or sample edges at all. This is a challenge for the theory and for the very scenario of chiral p-wave pairing. Difficulties with direct detection of ferromagnetism coexisting with superconductivity lead to the question of whether one may use the term *ferromagnetism* at all. Indeed in the literature sometimes they prefer to tell about *superconductivity with broken time-reversal symmetry* (TRS) as in the title of our Rapid Communication. However, one cannot imagine broken TRS without at least some features of ferromagnetism.

Among possible explanations why they cannot see stray fields from DWs is a domain structure with a period essentially smaller than a distance between a sample surface and a probe used by experimentalists. There were some pieces of experimental evidence of domains in both the spin SFs (Ref. 11) and the orbital SFs.[12] The theoretical investigations of the domain structure in SFs were restricted with the case of zero external magnetic field.[13–17] One must discern two possible types of equilibrium domain structure. The first one is well known for normal ferromagnets.[18] The domain structure results from competition between the energy of DWs and the magnetostatic energy of stray fields generated by the magnetic flux exiting from the sample surface. The period of the structure depends on the shape and the size of the sample going to infinity when the sample size grows. One can call these domains *extrinsic ferromagnetic domains*. Since in SFs the Meissner effect expels the magnetic field, it is impossible to benefit from decreasing the bulk magnetostatic energy in comparison with the DW energy, and extrinsic domains cannot appear at equilibrium.[15] But also long ago another type of domains was known, which decreases the bulk magnetostatic energy at the expense of destroying the Meissner state.[13,16,17] The size of these domains is roughly on the order of the London penetration depth λ and does not depend on either shape or size of the sample. Strictly speaking the state with this domain structure at the macroscopic scales is not ferromagnetic but antiferromagnetic though with a rather large period. We call such a state *cryptoferromagnetic*, the term introduced by Anderson and Suhl.[19]

This Rapid Communication analyzes the cryptoferromagnetic state in nonzero external magnetic field. We obtained the full phase diagram of both spin and orbital SFs with the phase transitions from the cryptoferromagnetic state to the Meissner and to the mixed states. Calculated magnetization curves demonstrate the absence of diamagnetism in the cryptoferromagnetic state. Measurements of magnetization curves can provide pieces of evidence of cryptoferromagnetism in superconductors with broken TRS.

Let us consider a stripe domain structure with 180° DWs in a sample subjected to external magnetic field $\mathbf{H}_0=(0,H_0,0)$. The DWs are parallel to the yz plane separating domains with alternating magnetization $\mathbf{M}=(0,\pm M,0)$. Since the $\mathbf{H}_0$ orientation is preferable the width $d_\uparrow$ of domains with the magnetization $\mathbf{M}$ parallel to $\mathbf{H}_0$ ($\uparrow$ domains) exceeds the width $d_\downarrow$ of the domains with $\mathbf{M}$ antiparallel to $\mathbf{H}_0$ ($\downarrow$ domains). We consider the case when the London penetration length λ exceeds the coherence length ξ and the DW thickness. Then the surface energy σ and the internal

structure of DW are not affected by fields and currents at scales of λ.

The Gibbs potential inside domains is

$$\mathcal{G} = \int d^3x \left(\frac{\mathbf{h}^2}{8\pi} + \frac{2\pi\lambda^2}{c^2}\mathbf{j}^2 - \mathbf{h}\cdot\mathbf{M} - \frac{\mathbf{h}\cdot\mathbf{H}_0}{4\pi} \right), \tag{1}$$

where $\mathbf{h}$ is the magnetic field, and $\mathbf{j}=(c/4\pi)\nabla\times\mathbf{h}$ is the electric current. Variation in the Gibbs potential yields the magnetic field $\mathbf{h}_{\uparrow,\downarrow}=(0,h_{\uparrow,\downarrow},0)$ in the $\uparrow$ domains and $\downarrow$ domains,

$$h_{\uparrow,\downarrow} = (H_0 \pm 4\pi M)\frac{\cosh(x/\lambda - \zeta_{\uparrow,\downarrow})}{\cosh\zeta_{\uparrow,\downarrow}}, \tag{2}$$

where x is the distance from the DW and $\zeta_{\uparrow,\downarrow}=d_{\uparrow,\downarrow}/2\lambda$. All fields are low compared to the upper critical field H_{c2}.

As shown in Ref. 20, for orbital ferromagnetism the spontaneous magnetization cannot be defined unambiguously and the Landau-Lifshitz theory of ferromagnetism[18] based on this definition is not valid. Nevertheless, interaction of magnetization currents inside narrow DW with the magnetic field can be reduced to the expression looking like the standard Zeeman energy $-\mathbf{h}\cdot\mathbf{M}$. However, here $\mathbf{M}$ is not a magnetic moment inside the domain but is defined so that $8\pi M$ was the jump of the magnetic field on the DW [see Eq. (2)]. So "magnetization" M is determined by the DW structure and cannot be used for other phenomena connected with ferromagnetic ordering, e.g., analyzing the magnon spectrum.[20]

Substituting Eq. (2) into Eq. (1), adding the surface energy σ of DWs, and averaging over the domain-structure period $d=d_\uparrow+d_\downarrow$ we obtain the reduced energy density $\mathcal{E}=\mathcal{G}/2\pi M^2 V$ (V is the sample volume);

$$\mathcal{E} = \frac{2w - (1+h_0)^2\tanh\zeta_\uparrow - (1-h_0)^2\tanh\zeta_\downarrow}{\zeta_\uparrow + \zeta_\downarrow}. \tag{3}$$

Here $h_0=H_0/4\pi M$ and $w=\sigma/4\pi M^2\lambda$ are dimensionless parameters.

Minimization of energy density in Eq. (3) with respect to $\zeta_\uparrow$ and $\zeta_\downarrow$ yields two nonlinear equations for $\zeta_\uparrow$ and $\zeta_\downarrow$,

$$\tanh\frac{\zeta_\uparrow - \zeta_\downarrow}{2}\tanh\frac{\zeta_\uparrow + \zeta_\downarrow}{2} = h_0,$$

$$\frac{\sinh 2\zeta_\uparrow + \sinh 2\zeta_\downarrow - 2(\zeta_\uparrow + \zeta_\downarrow)}{(\cosh\zeta_\uparrow + \cosh\zeta_\downarrow)^2} = w. \tag{4}$$

The magnetic induction $\mathbf{B}=\langle\mathbf{h}\rangle$ is determined by reduced magnetic induction $b=B/4\pi M$,

$$b = -\frac{1}{2}\frac{\partial\mathcal{E}}{\partial h_0} = \frac{(1+h_0)\tanh\zeta_\uparrow - (1-h_0)\tanh\zeta_\downarrow}{\zeta_\uparrow + \zeta_\downarrow}. \tag{5}$$

Figure 1(a) shows the phase diagram in the plane w^2-h_0. The area of the cryptoferromagnetic state is restricted by two lines where the phase transition between the cryptoferromagnetic and the Meissner states occurs:

(1) The line $\mathcal{E}=0$, which corresponds to the limit $\zeta\to\infty$, where $\zeta=\zeta_\uparrow+\zeta_\downarrow$ is a period of domain structure. The values of w and h_0 on this line are connected by the relation $w=1+h_0^2$.

(2) The line on which domains with magnetization opposite to the external magnetic field vanish; $\zeta_\downarrow=0$. The equation describing this line is

$$w_c = \sqrt{h_c}(1+h_c) - \frac{(1-h_c)^2}{2}\ln\frac{1+\sqrt{h_c}}{1-\sqrt{h_c}}, \tag{6}$$

with the critical size of the $\uparrow$ domain being

$$\zeta_{\uparrow c} = \ln\frac{1+\sqrt{h_c}}{1-\sqrt{h_c}}. \tag{7}$$

The magnetic induction on the critical line is

$$b_c = 2\sqrt{h_c}\left(\ln\frac{1+\sqrt{h_c}}{1-\sqrt{h_c}}\right)^{-1}. \tag{8}$$

At the left lower corner of the diagram ($w\ll 1$ and $h_0\ll 1$), the critical parameters on the line $\zeta_\downarrow=0$ are

$$h_c = \frac{1}{4}(3w)^{2/3}, \quad \zeta_{\uparrow c} = (3w)^{1/3}. \tag{9}$$

Aside from the critical line Eq. (4) yields

$$h_0 = \frac{\zeta_\uparrow^2 - \zeta_\downarrow^2}{4}, \quad w = \frac{\zeta_\uparrow^3 + \zeta_\downarrow^3}{3}. \tag{10}$$

For small $h_0\ll h_c$ one can solve Eq. (10) analytically as

$$\zeta_{\uparrow,\downarrow} = 4^{1/3}\sqrt{h_c}\left(1 - \frac{h_0^2}{4^{4/3}h_c^2}\right) \pm \frac{h_0}{4^{1/3}\sqrt{h_c}}. \tag{11}$$

Up to now we ignored the possibility of the transition to the mixed state assuming that the first critical magnetic field $H_{c1}=\Phi_0\ln\kappa/4\pi\lambda^2$ essentially exceeds the characteristic fields of the cryptoferromagnetic state. Here Φ_0 is flux quanta and $\kappa=\lambda/\xi$. Both the field H_{c1} and the parameter w depend on the penetration depth λ, and it is useful to introduce the reduced first critical field $h_{c1}=H_{c1}/4\pi M w^2=\Phi_0 M^3\ln\kappa/\sigma^2$, which does not depend on λ. The reduced free energy of the mixed state with respect to the energy of the Meissner state is

$$\mathcal{E}_m = -\left(1 + h_0 - \frac{H^*}{4\pi M}\right)^2 = -(1 + h_0 - h_{c1}w^2)^2, \tag{12}$$

where the field H^* inside the mixed state differs from H_{c1} by another logarithm factor, but we neglect it assuming $H^*\approx H_{c1}$. Equation (12) takes into account the presence of the spontaneous magnetization and the order-parameter gradients related to vorticity.[21] In the cryptoferromagnetic state the gradient terms also contribute to the DW surface energy σ.

The phase transition to the mixed state may occur either from the Meissner state being determined by the condition $\mathcal{E}_m=0$ (the second-order transition) or from the cryptoferromagnetic state crossing the critical line on which $\mathcal{E}_m=\mathcal{E}$ (the first-order transition). At zero external field h_0 and small w the phase transition between the mixed state and the cryptoferromagnetic state occurs at $w_m\approx\sqrt{3}/(2h_{c1})^{3/4}$. Thus however large h_{c1} is, at the left lower corner of the phase diagram there is always *the spontaneous vortex phase*, i.e., the mixed

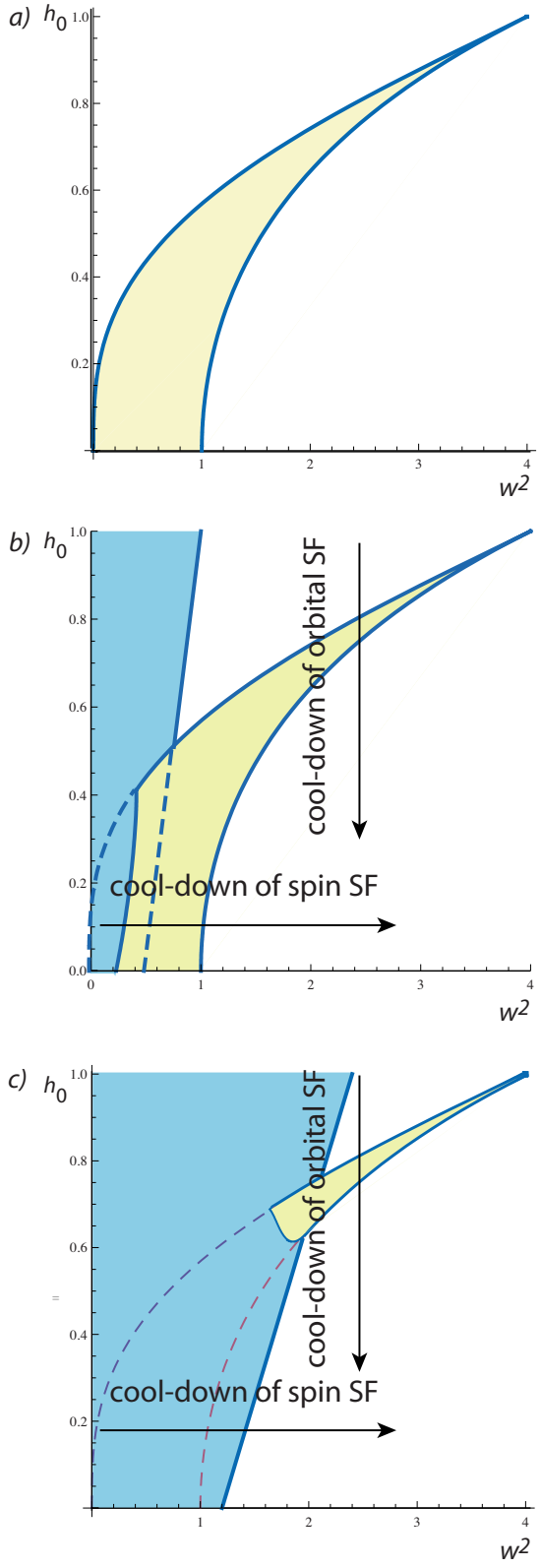

FIG. 1. (Color online) Phase diagram for various values of the reduced lower critical field h_{c1}: (a) $h_{c1}\to\infty$; (b) $h_{c1}=2$; and (c) $h_{c1}=0.83$. The lighter shaded (yellow) area is the cryptoferromagnetic state. The darker shaded (blue) area is the mixed state. The rest is the Meissner state. The horizontal and the vertical arrows show the processes of field cooling across the SC critical temperature of spin and orbital SFs, respectively.

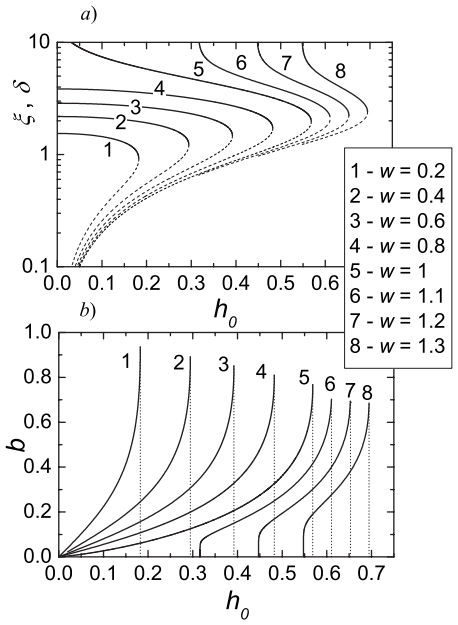

FIG. 2. (a) Magnetic field dependencies of $\zeta=\zeta(h_0)$ (solid line) and $\delta=\delta(h_0)$ (dashed line), and (b) magnetization curves are shown at different values of parameter w. Vertical lines correspond to critical fields above which the intrinsic domain structure collapses.

state without external magnetic field. The full phase diagrams at two finite values $h_{c1}=2$ and 0.83 are shown in Figs. 1(b) and 1(c). The cryptoferromagnetic state disappears from the phase diagram at $h_{c1}<0.5$. Our phase diagram did not include a possible phase with coexisting vortices and domains. Preliminary estimations show that this phase can appear in the area of the mixed state in Fig. 1 but does not affect the area occupied by the cryptoferromagnetic phase, which is the main goal of the present work. Studying of the state with domains and vortices requires the analysis of the stability of the mixed state with respect to domainization and should be done elsewhere.

Figure 2(a) shows the period $\zeta=\zeta_\uparrow+\zeta_\downarrow$ and the difference of the two domain widths $\delta=\zeta_\uparrow-\zeta_\downarrow$ as functions of the reduced magnetic field h_0. The magnetization curves $b(h_0)$, which were calculated numerically, are shown in Fig. 2(b). The linear magnetic permeability as a function of w is determined from the following two relations ($\zeta=2\zeta_\uparrow=2\zeta_\downarrow$):

$$\mu=\frac{db}{dh_0}=\frac{\coth\zeta}{\zeta},\quad w=\tanh\zeta-\frac{\zeta}{\cosh\zeta}. \tag{13}$$

At $w\to 0$ the permeability is divergent: $\mu\approx(2/3w)^{2/3}$. In contrast to other states in the diagram, at $w<1$ the cryptoferromagnetic state is a pure paramagnetic.

The sequence of phase transformations in the process of field cooling below the SC critical temperature is different for spin and orbital SFs. In spin SFs, where the magnetic transition occurs at much higher temperature, one may neglect temperature dependence of M, σ, and h_{c1}. Then only $w^2\propto 1/\lambda^2\propto\tau$ depends on relative temperature difference $\tau=(T_c-T)/T_c$. On the phase diagrams of Figs. 1(b) and 1(c) the state moves along straight lines parallel to the horizontal

axis w^2. From these figures it is evident that just below the critical temperature the system enters the mixed state. At further cooling down the system crosses to the Meissner state either directly or through the area of the cryptoferromagnetic state. For orbital SFs the cooling process occurs differently. In this case the magnetization $M \sim \Phi_0/\lambda^2 \propto \tau$ and the DW surface energy is a product of the condensation energy $H_c^2(\tau) \sim [\Phi_0/\lambda(\tau)\xi(\tau)]^2$ and the coherence length $\xi(\tau) \sim \xi_0/\sqrt{\tau}$: $\sigma \sim \tau^{3/2}\Phi_0^2/\lambda_0^2\xi_0$. Here λ_0 and ξ_0 are the penetration depth and the coherence length at zero temperature. Then the parameters $w^2 \sim h_{c1}^{-1} \sim (\lambda_0/\xi_0)^2$ do not depend on temperature whereas the reduced magnetic field does: $h_0 = H_0/4\pi M \propto 1/\tau$. Thus in the field-cooling process the state moves along vertical lines on the phase diagrams in Figs. 1(b) and 1(c). However, as pointed out above, the cryptoferromagnetic state can compete with the mixed state only if h_{c1} is high enough. Since $h_{c1} \sim (\xi_0/\lambda_0)^2$, this requires λ_0 not to be large compared to ξ_0. In Sr_2RuO_4 according to Ref. 10 the ratio of $\lambda_0 = 190$ nm to $\xi_0 = 66$ nm is not too high indeed. But this means that the DW thickness is not so small compared to λ as assumed in our analysis. Therefore for orbital SFs our analysis can provide only a qualitative but still credible picture of the phase transformations.

In conclusion, we analyzed the phase diagram of superconductors with a broken time-reversal symmetry in which superconductivity competes either with spin ferromagnetism or with ferromagnetism originated from the intrinsic angular momentum of Cooper pairs (chiral p-wave superconductors such as Sr_2RuO_4). The phase diagram includes the state with the intrinsic domain structure, which has no ferromagnetic order at macroscopic scales and therefore called cryptoferromagnetic. The cryptoferromagnetic state is not diamagnetic, either fully (as the Meissner state) or partially (as the mixed state). The state can be detected experimentally with detailed measurements of magnetization curves.

This work was supported by the grant of the Israel Academy of Sciences and Humanities.

[1] I. Felner, U. Asaf, Y. Levi, and O. Millo, Phys. Rev. B **55**, R3374 (1997).
[2] M. R. Eskildsen, K. Harada, P. L. Gammel, A. B. Abrahamsen, N. H. Andersen, G. Ernst, A. P. Ramirez, D. J. Bishop, K. Mortensen, D. G. Naugle, K. D. D. Rathnayaka, and P. C. Canfield, Nature (London) **393**, 242 (1998).
[3] G. M. Luke, Y. Fudamoto, K. M. Kojima, M. I. Larkin, J. Merrin, B. Nachumi, Y. J. Uemura, Y. Maeno, Z. Q. Mao, Y. Mori, H. Nakamura, and M. Sigrist, Nature (London) **394**, 558 (1998).
[4] K. Ishida, H. Mukuda, Y. Kitaoka, K. Asayama, Z. Q. Mao, Y. Mori, and Y. Maeno, Nature (London) **396**, 658 (1998).
[5] S. S. Saxena, P. Agarwal, K. Ahilan, F. M. Grosche, R. K. W. Haselwimmer, M. J. Steiner, E. Pugh, I. R. Walker, S. R. Julian, P. Monthoux, G. G. Lonzarich, A. Huxley, I. Sheikin, D. Braithwaite, and J. Flouquet, Nature (London) **406**, 587 (2000).
[6] C. Pfleiderer, M. Uhlarz, S. M. Hayden, R. Vollmer, H. v. Löhneysen, N. R. Bernhoeft, and G. G. Lonzarich, Nature (London) **412**, 58 (2001).
[7] A. P. Mackenzie and Y. Maeno, Rev. Mod. Phys. **75**, 657 (2003).
[8] J. Xia, Y. Maeno, P. T. Beyersdorf, M. M. Fejer, and A. Kapitulnik, Phys. Rev. Lett. **97**, 167002 (2006).
[9] C. Day, Phys. Today **59**(12), 23 (2006).
[10] J. R. Kirtley, C. Kallin, C. W. Hicks, E.-A. Kim, Y. Liu, K. A. Moler, Y. Maeno, and K. D. Nelson, Phys. Rev. B **76**, 014526 (2007).
[11] G. I. Leviev, M. I. Tsindlekht, E. B. Sonin, and I. Felner, Phys. Rev. B **70**, 212503 (2004).
[12] F. Kidwingira, J. D. Strand, D. J. Van Harlingen, and Y. Maeno, Science **314**, 1267 (2006).
[13] U. Krey, Int. J. Magn. **3**, 65 (1972).
[14] L. N. Bulaevskii, A. I. Buzdin, and S. S. Crotov, Solid State Commun. **48**, 719 (1983).
[15] E. B. Sonin, Phys. Rev. B **66**, 100504(R) (2002).
[16] M. Fauré and A. I. Buzdin, Phys. Rev. Lett. **94**, 187202 (2005).
[17] E. B. Sonin, Phys. Rev. Lett. **95**, 269701 (2005); M. Fauré and A. I. Buzdin, *ibid.* **95**, 269702 (2005).
[18] L. D. Landau and E. M. Lifshitz, *Electrodynamics of Continuous Media* (Pergamon, Oxford, 1984).
[19] P. W. Anderson and H. Suhl, Phys. Rev. **116**, 898 (1959).
[20] V. Braude and E. B. Sonin, Phys. Rev. B **74**, 064501 (2006).
[21] E. B. Sonin and I. Felner, Phys. Rev. B **57**, R14000 (1998).